

钛/铝爆炸焊界面形成机制数值模拟与试验验证

李岩^{1,2}, 李艳彪¹, 刘翠荣¹, 任金锁², 赵瑞²

(1. 太原科技大学, 太原 030024; 2. 山西阳煤化工机械(集团)有限公司, 太原 030032)

摘要: 以爆炸焊制备钛/铝复合板为例, 利用数值模拟再现爆炸焊瞬态成形过程, 并通过试验分析爆炸焊界面特征。结果表明, 由于射流的侵彻作用, 沿爆轰波传播方向, 钛/铝复合板结合界面由平直结合向波形结合转变。起爆点处压力较小, 出现边界效应。爆炸焊撞击区极高的碰撞压力, 是促使界面产生塑性变及晶粒细化的原因。高速冲击导致爆炸焊界面缺陷增多, 这为原子的扩散提供了通道, 从而使钛、铝在界面产生互扩散, 实现冶金结合。数值模拟结果与试验结果相吻合, 揭示了钛/铝爆炸焊界面的形成机制。

关键词: 波纹管; 钛/铝复合板; 爆炸焊; 界面成形机制; 数值模拟

中图分类号: TG456.6

0 前言

爆炸焊是集动力学、热力学、材料学等多学科交叉的特种焊接方法, 其具有高效、低成本、适用性广的特点, 在层状金属复合材料制造领域被应用广泛^[1-2]。爆炸焊从发现至今已有 70 余年的历史, 目前有近 260 种同种或异种金属或非金属复合材料可以用爆炸焊技术制备^[3], 爆炸焊研究一直没有退出人们的视野。爆炸焊界面是异种材料成分、组织、性能的过渡区, 是决定复合材料服役寿命的关键部位^[4-5]。爆炸焊在高温、高压下瞬间完成, 基于目前的试验条件, 难以控制并实时观测到爆炸焊成形瞬态过程。爆炸焊界面瞬态形成机理及其对复合材料产品质量的影响等仍未能得到令人满意的解释。

随着计算机软、硬件的发展和数值算法的进步, 数值模拟技术为再现爆炸焊瞬态成形过程提供了可能^[6]。利用数值模拟技术从爆炸焊成形特征出发, 分析爆炸焊结合区特征, 对制备高质量的爆炸焊复合材料有重要的理论和工程实践意义。

目前, 在关于爆炸焊的数值模拟中, 通常是基于一维格尼公式将爆炸焊过程看作高速碰撞问题处理^[7-9]。实际的爆炸焊起爆后, 覆板被爆轰波折弯, 与

基板发生倾斜碰撞。基于一维格尼公式的高速倾斜碰撞模型不能在现爆轰波传播过程和覆板动态折弯的过程。因此, 为了更加真实地再现爆炸焊瞬态成形过程, 文中建立由炸药、覆板、基板、地基 4 部分组成的爆炸焊模型, 以重现完整的爆炸焊成形过程。

文中以爆炸焊制备钛/铝复合板为例, 利用 ANSYS/AUTODYN 非线性显式动力学软件建立了钛/铝爆炸焊 2D 数值仿真模型, 应用光滑粒子流体动力学方法 (SPH) 和任意拉格朗日 - 欧拉法 (ALE) 再现了钛/铝复合板爆炸瞬态成形特征。进行钛/铝爆炸焊试验, 并利用先进材料分析手段, 表征分析爆炸焊界面特征。数值模拟与试验分析相结合, 揭示钛/铝爆炸焊界面的形成机制。

1 试验材料及方法

以 1 mm TA1 钛板为复层, 3 mm Al-1060 铝板为基层, 用爆炸焊方法制备钛/铝层状复合材料, 材料成分见表 1 和表 2。爆炸焊采用平行安装的方式, 选用膨化硝酸混合炸药, 密度 790 kg/mm³, 理论爆炸速度 2 400 m/s, 炸药厚度 5 mm, 基板 - 覆板间隙 4 mm, 采用边缘引爆。

采用慢走丝线切割沿爆轰波传播的方向切取钛/铝复合材料横截面来制备金相试块。在基恩士 (VHX-2000) 超景深显微镜下观察钛/铝复合材料界面结合形貌。蔡司 SIGMA 扫描电镜 (SEM), 配牛津能谱仪 (EDS) 对界面元素进行分析。采用电解抛光制取界面 EBSD 试样, 牛津 EBSD 表征, Channel 5 软件进行数据处理。根据 GB/T 4340.1—2009《金属材料 维氏硬度

收稿日期: 2021-06-02

基金项目: 国家重点研发计划(20180707305); 山西省高等学校科技创新项目资助(20190615); 山西省青年科学基金(201901211291); 太原科技大学博士启动资金(20182041, 20192011)。

doi: 10.12073/j.hj.20210602002

表1 TA1的化学成分(质量分数,%)

Si	Fe	C	N	H	O	Ti
0.1	0.15	0.05	0.03	0.015	0.15	余量

表2 Al-1060的化学成分(质量分数,%)

Si	Fe	Cu	Mn	Mg	Cr	Ni	Zn	Ti	Al
0.12	0.32	<0.01	<0.01	<0.01	<0.01	<0.01	<0.01	0.02	余量

试验第1部分:试验方法》,利用HV-1000B显微硬度测试仪沿着垂直于复合板界面方向,测试界面附近显微硬度值。

2 数值模拟建模

运用ANSYS/AUTODYN建立钛/铝爆炸焊过程2D计算模型。图1是钛/铝爆炸焊2D数值仿真模型,模型包括炸药20 mm×5 mm、覆板(Ti)20 mm×1 mm、基板(Al)20 mm×3 mm、地基25 mm×8 mm,基板-覆板间隙4 mm,设置边缘起爆(起爆点)。在基板(Al)上表面取等距离间隔的特征点1~6,在覆板(Ti)下表面取等距离间隔的特征点7~12。地基采用固定边界条件,其它物体设置为自由边界条件。

模拟中炸药选用Jones-Wilkins-Lee(JWL)状态方程,基板和覆板均选用Johnson-Cook本构方程和Mie-Gruneisen状态方程^[10]。选用SPH法模拟基板和覆板,选用ALE模拟炸药和地基。

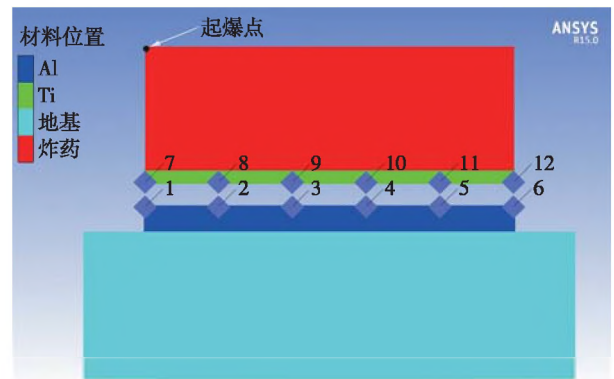


图1 钛/铝爆炸焊2D模型

SPH法粒子的大小对模拟结果及可视化分析有重要的影响,经过多次调试和参考同类文献的基础上^[7],在该次模拟中,SPH法粒子的大小 Δr 设置为20 μm ,模型中共包含56 250个粒子,ALE网格尺寸设置为0.1 mm。炸药和材料的相关参数分别见表3^[10]和表4^[10]。

表3 炸药的计算参数

爆炸速度 $v/(\text{m} \cdot \text{s}^{-1})$	炸药密度 $\rho/(\text{kg} \cdot \text{m}^{-3})$	炸药总能量 E_0/GJ	常数 A/GJ	常数 B/GJ	常数 R_1	常数 R_2	常数 ω
2 400	790	2.48	491	0.89	3.9	1.18	0.33

表4 材料的状态方程和本构模型参数

材料	密度 $\rho/(\text{kg} \cdot \text{m}^{-3})$	屈服应力 R/MPa	应变硬化系数 β/MPa	应变率相关系数 C	温度相关系数 m	应变硬化指数 n	熔点 $T_m/^\circ\text{C}$	抗剪强度 R_s/GPa	抗压强度 Y_0/GPa
钛板	4 520	2 500	150	0.03	0.8	0.32	1 660	55	0.16
铝板	2 770	3 600	30	0.01	1	0.41	660	27	0.04
地基	7 896	7 000	3 290	0.22	1	0.36	1 811	81.8	0.35

3 结果分析

3.1 爆炸焊瞬态成形及界面形态

图2是钛/铝复合板爆炸焊成形过程。图2a是初始安装 $t=0$ 时刻,炸药未起爆,钛板和铝板平行放置;图2b是爆轰 $t=1.04 \times 10^{-6}$ s时刻,当炸药从左端起爆后,产生爆轰波,爆轰波向右传播,爆轰产物急剧向四

周膨胀,爆轰波掠过的瞬间,覆板受到突跃的强激波作用,覆板在爆轰波的作用下被折弯,通过间隙加速后,与基板发生倾斜碰撞,在结合区未见界面处有射流产生,且结合界面为平直状;随着爆轰波的传播,碰撞点不断向前推进,在 $t=3.23 \times 10^{-6}$ s时刻,如图2c所示,界面处出现射流,在结合面形成波形结合。由图2的模拟结果知,在爆炸焊中,射流并未在基板、覆板初始

碰撞的时刻产生,而是随着爆炸复合进行才出现射流,分析其主要原因:爆炸焊试验采用平行安装的复合方式,初始时刻,基板和覆板平行放置,无初始安装角,

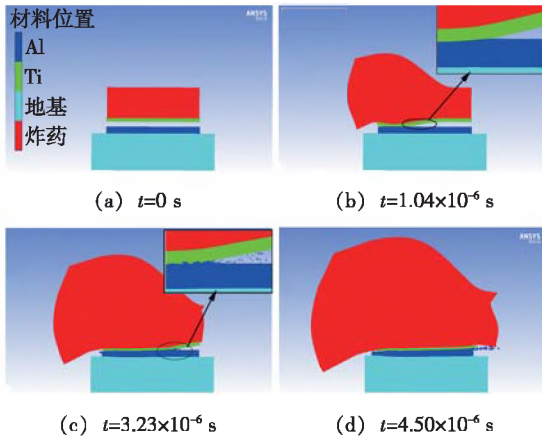


图2 爆炸焊过程模拟

随着爆炸焊进行,撞击角达到一定的范围时射流会产生。模拟结果与文献[11-12]的论述相一致。

图3是沿爆轰波传播的方向,起爆点、靠近起爆点、远离起爆点3个位置钛/铝界面形貌。对比试验与模拟结果发现,在起爆点附近(a位置)钛板和铝板没有实现复合,下文将详细分析未复合原因。在离起爆点不远的位置(b位置)钛/铝界面呈现平直形貌,无裂纹、气孔等冶金缺陷;在离起爆点更远的位置(c位置),钛/铝界面呈现波状形貌,图4是爆炸焊界面的波纹形貌。界面结合形态,试验结果和模拟结果相吻合,这也进一步验证了数值模型的准确性。图5是速度场云图,模拟结果表明撞击区射流的喷射速度最高可达7000 m/s,射流极高的喷射速度为清除待结合表面的氧化薄膜和污渍,瞬间的清洗形成了新鲜的表面,为原子间的结合提供了必要的条件。

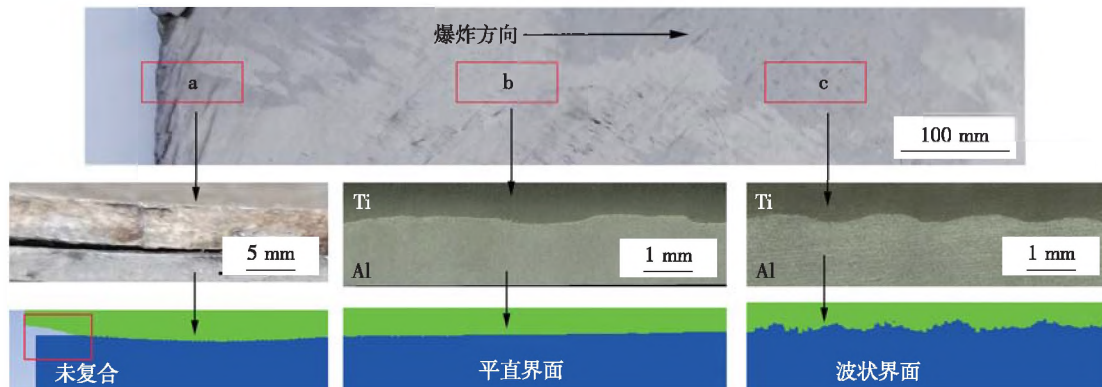


图3 试验与模拟钛/铝爆炸焊界面形态

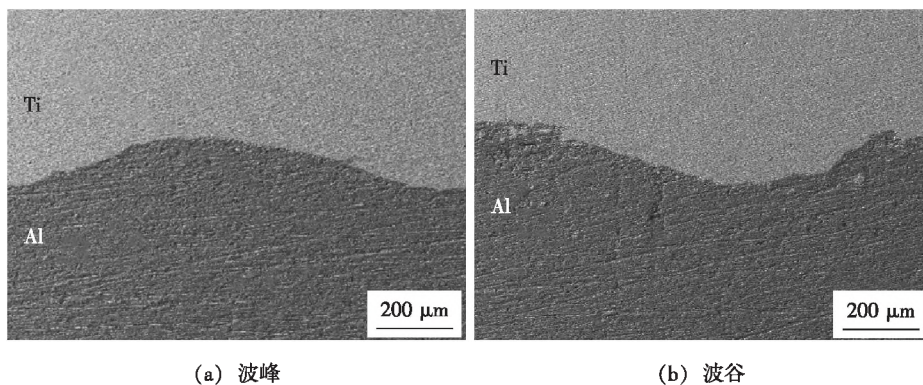


图4 爆炸焊界面的波纹形貌

结合图1和图2分析可以看出,基板、覆板碰撞初期并未有射流产生,界面为平直状,随着复合的进行,碰撞角变大,射流产生并出现波形结合界面,这一点恰好验证了Bahrani等人提出的射流侵彻机理^[12],即射流可以看作是低粘性流体,在高压的侵彻作用下,材料发生变形,形成凸起,凸起不断升高俘获射流,碰撞点

不断向前推进,形成下一个波形,如此往复形成连续性的波状界面。

3.2 爆炸焊界面塑性变形

图6是钛/铝爆炸焊成形某时刻有效塑性应变云图。在钛/铝结合区界面产生了一条明显的塑性变形带,且塑性应变带呈现波状结合形态。模拟结果表明,

钛/铝爆炸焊界面产生了严重的塑性变形。模拟结果与 EBSD 测试得到的钛/铝爆炸焊界面应变结果一致,如图 7 所示。

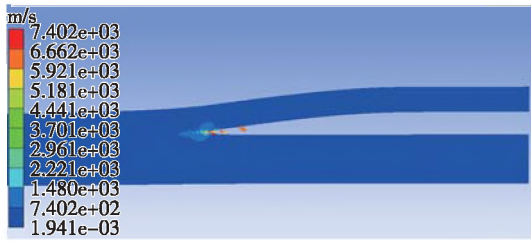


图 5 速度场云图

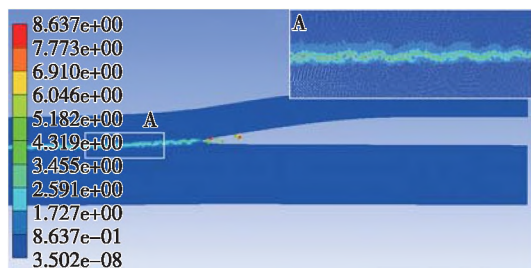


图 6 有效塑性应变云图

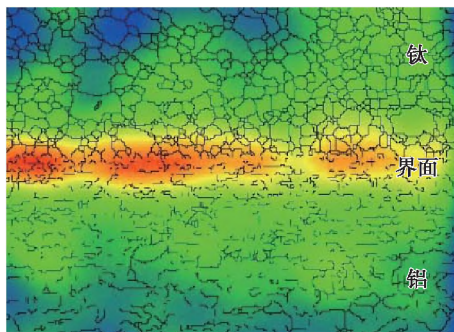


图 7 钛/铝界面 EBSD 应变图

图 8 是特征点 3 和特征点 9 爆炸成形过程塑性应变随时间变化的曲线。在 $t = 2.2 \times 10^{-6}$ s 时刻,特征点 3 和特征点 9 有效塑性应变值突然增大然后趋于平稳,这是由于覆板上炸药所产生的爆轰波使碰撞点产生了高的速度和高的压力,瞬时极高的压力和速度在界面处产生了大的塑性变形。随时间增加,有效塑性应变趋于平稳,证实了爆炸冲击产生的塑性变形是不可逆的。另外,钛板下表面特征点 9 最大有效塑性应变值为 2.2,铝板上表面特征点 3 最大有效塑性应变值为 2.8,这是由于铝比钛软,更容易产生变形造成的。

图 9 是钛/铝界面显微硬度分布图。沿钛/铝复合板界面垂直的方向,界面附近显微硬度增大,这是由于在爆轰波的作用下,2 种材料待结合界面高速撞击,产

生了严重的塑性变形,这一现象由模拟结果可以解释。界面位置钛的硬度最大,可达到 210 HV,比母材 140 HV 增大 70%,铝侧最大硬度为 60 HV,比母材 33 HV 增大 81%。说明铝侧产生的塑性变形更大,这与特征点 3 和特征点 9 最大有效塑性应变值是一致的。

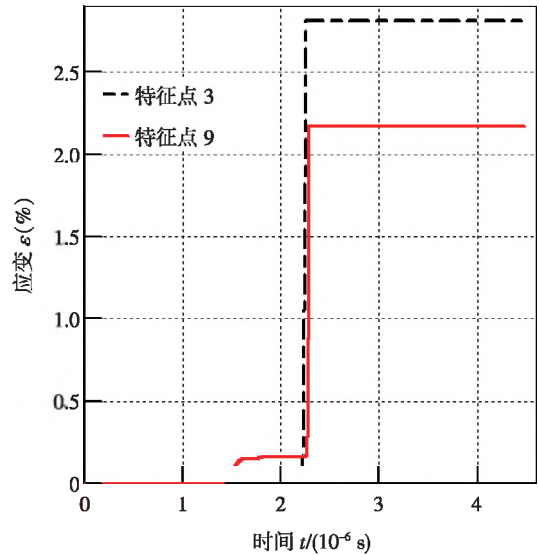


图 8 特征点 3 和特征点 9 有效塑性变形—时间曲线

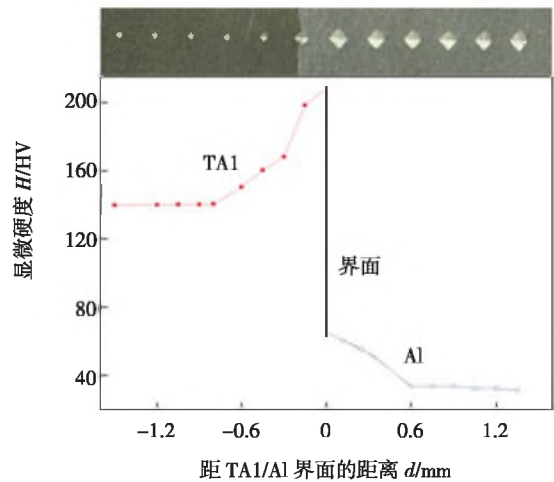


图 9 爆炸焊钛/铝界面附近显微硬度

3.3 爆炸焊界面晶粒细化

图 10 是钛/铝爆炸焊过程中某一时刻界面区压力云图,模拟结果显示,撞击区域的压力最大,且压力场呈不对称分布,压力场不对称分布与材料自身的物理性质有关,相关文献报道,当同种材料爆炸复合时,撞击区压力呈对称分布^[7]。撞击面要产生射流所需的压力必须超过材料的动态屈服强度,材料的动态屈服极限为材料静态屈服强度的 10 ~ 12 倍^[13-14]。在该次模拟中,撞击区最大压力为 29.8 GPa,远远大于钛、铝 2

种材料的动态屈服极限,因此在撞击界面位置产生了射流。撞击区压力远大于材料的动态屈服极限也可以解释界面产生大塑性变形的试验现象。

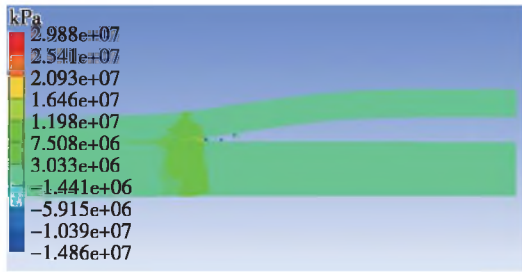


图10 压力分布云图

图11是特征点在整个爆炸焊过程中压力随时间变化的曲线。由图可知,沿着爆轰波传播的方向,起爆位置特征点1和特征点7位置压力为零。起爆点位置由于炸药稀疏波作用,炸药引爆后要在一定时间内才能达到稳定的爆轰^[15-16]。特征点1位置压力极低与起爆点位置炸药未能达到稳定爆轰有关。由图3钛/铝爆炸焊界面可知,在起爆点位置模拟和试验结果均显示,起爆点位置界面未复合。起爆点特征点1位置产生的压力小,爆轰载荷所未能使覆板折弯,从而不能与特征点7发生撞击。由此可见,起爆点压力值较低是爆炸焊边界效应产生的本质原因。因此,爆炸焊复合板生产企业一直沿用在起爆点位置添加黑火金高能炸药,使边界部位尽快达到爆轰稳定,以减少爆炸焊边界效应。

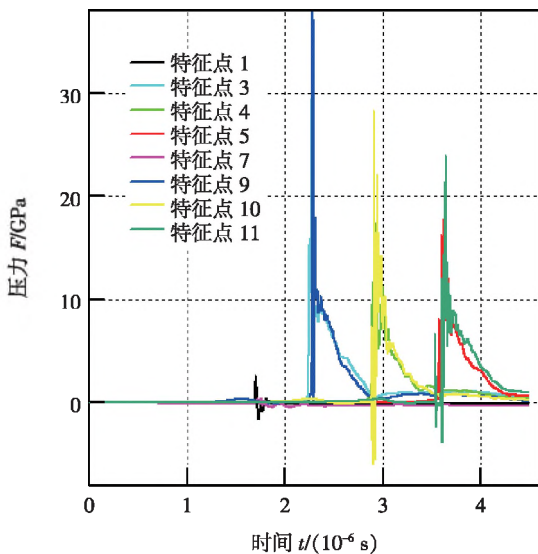


图11 特征点压力—时间曲线

根据图11,起爆后 2.2×10^{-6} s时刻,特征点3和特征点9的压力值呈脉冲状的上升趋势,说明此刻特征点3和特征点9发生碰撞,随后2点压力曲线重合,

说明2撞击点实现结合,2对撞点压力由峰值逐渐下降,约 0.8×10^{-6} s后,下降到零。随着爆轰波向前传播,其他撞击点压力—时间曲线呈现出类似的变化情况,压力峰值较为接近,达10 GPa数量级,极高的压力促使待焊接表面原子之间的距离达到引力范围之内,从而实现钛铝材料的焊接。

图12为试验获得的钛/铝爆炸焊界面EBSD晶粒尺寸统计图,钛/铝爆炸焊界面存在明显的晶粒细化现象。这是由于爆炸焊极高的碰撞压力,促使原始晶粒破碎而形成的。随着距界面位置的增加,母材所受的碰撞压力作用力逐渐减弱,因此,在远离界面位置晶粒未发生细化,保留原始的形态。

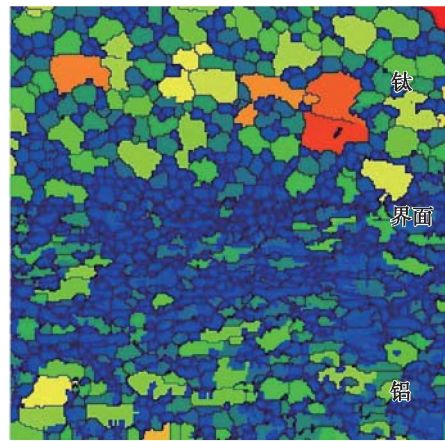


图12 钛/铝爆炸焊界面EBSD图像

3.4 爆炸焊界面元素扩散

图13是试验获得的垂直钛/铝爆炸焊界面EDS线扫描图。钛/铝爆炸焊复合材料界面处,两元素扩散曲线呈现“X”状,2种原子的含量存在连续、平稳的过渡,说明在爆炸焊过程中Ti元素和Al元素发生了互扩散,2种金属达到了扩散冶金结合。

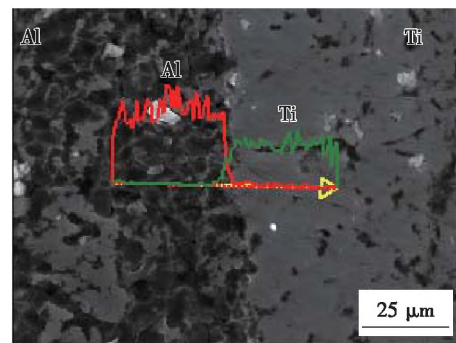


图13 钛/铝爆炸焊界面元素线扫描

由上述数值模拟结果知,在爆炸焊过程中,覆板在爆轰波作用下,与基板发生高速倾斜碰撞,界面处于高

压(约 10 GPa 数量级)、大塑性变形(有效塑性变形大于 2)条件,高压、大变形消除了待结合区表面晶格微观缺陷,缩小了原子间距,使 2 原子之间产生键合力,有利于界面元素的相互扩散。另外,由 EBSD 试验结果可以看出爆炸焊界面晶粒细化,晶界增多,另外,在强烈的外部作用力条件下,爆炸焊界面位置晶粒易产生大量的位错^[17],晶体缺陷处点阵畸变较大,原子处于较高的能量状态,易于跳跃,而位错和晶界等缺陷位置扩散激活能是晶格内扩散激活能的 1/2 ~ 1/3,晶界、位错等对扩散起着快速的通道作用^[18],这将加速了钛、铝 2 种元素的互扩散。原子的扩散,有利于增强原子间的相互结合力,从而增加 2 种材料结合强度。

4 结论

(1) 钛/铝爆炸焊界面形态的数值模拟结果与试验观察结果相一致,沿爆轰波传播方向,钛/铝复合板结合界面由平直结合向波形结合转变。起爆点处由于稀疏波的作用,导致起爆点位置压力较小,出现边界效应。

(2) 钛/铝爆炸焊界面显微硬度测试结果表明,爆炸焊界面存在加工硬化。模拟结果表明,炸药所产生的爆轰波使碰撞点产生高的压力,撞击区压力值可达 10 GPa 数量级,在钛/铝爆炸焊界面产生明显的塑性变形带,解释了试验中界面显微硬度测试结果。

(3) 钛/铝爆炸焊界面 EBSD 测试结果表明爆炸焊界面晶粒出现明显细化,爆炸焊极高的碰撞压力,是促使原始晶粒破碎导致晶粒细化的原因之一。

(4) 钛/铝爆炸焊界面 EDS 线扫描表明,钛、铝 2 种元素在结合区发生了明显的互扩散。爆炸焊时,覆板和基板高速倾斜碰撞,界面处于高压、大塑性变形条件下,导致界面位错和晶界等缺陷增多,为原子的扩散提供了通道,从而使钛、铝在界面发生互扩散,实现冶金结合。

参考文献

- [1] 郑远谋. 爆炸焊接和金属复合材料及其工程应用[M]. 长沙:中南大学出版社, 2002.
- [2] 孙泽瑞, 史长根, 吴晓明, 等. 双立爆炸大板面 TA2/Q235B 复合板宏观变形初探[J]. 焊接, 2020(8): 1-8.
- [3] Qi Junxiang, Miao Guanghong, Ai Jiuying, et al. Study on numerical simulation of TA1-304 stainless steel explosive welding [J]. China Welding, 2021, 30(2): 11-16.
- [4] Fronczek D M, Chulist R, Litynska-Dobrzynska L, et al. Microstructure changes and phase growth occurring at the interface of the Al/Ti explosively welded and annealed joints [J]. Journal of Materials Engineering and Performance, 2016, 25(8): 3211-3217.
- [5] Xia H B, Wang S G, Ben H F. Microstructure and mechanical properties of Ti/Al explosive cladding[J]. Materials & Design, 2014, 56: 1014-1019.
- [6] Li Y, Liu C, Yu H, et al. Numerical simulation of Ti/Al bimetal composite fabricated by explosive welding[J]. Metals, 2017, 7(10): 1-13.
- [7] Nassiri A, Kinsey B. Numerical studies on high-velocity impact welding: smoothed particle hydrodynamics (SPH) and arbitrary lagrangian-eulerian (ALE) [J]. Journal of Manufacturing Processes, 2016, 24(Part 2): 376-381.
- [8] Yuan X D, Wang W X, Cao X Q, et al. Numerical study on the interfacial behavior of Mg/Al plate in explosive/impact welding [J]. Science and Engineering of Composite Materials, 2015, 24(4): 2328-2335.
- [9] Mousavi A A A, Al-Hassani S T S. Numerical and experimental studies of the mechanism of the wavy interface formations in explosive/impact welding [J]. Journal of the Mechanics & Physics of Solids, 2005, 53(11): 2501-2528.
- [10] Autodyn. SPH user manuals & tutorial (revision 4.3) [M]. Century Dynamics, Inc., USA, 2007.
- [11] 唐文龙. 不锈钢/钢复合板的爆炸焊接试验与数值模拟 [D]. 南京:南京理工大学硕士学位论文, 2013.
- [12] 王道阳. 铝-钢复合管爆炸焊接数值模拟及实验研究 [D]. 安徽淮南:安徽理工大学硕士学位论文, 2016.
- [13] Li X J, Mo F, Wang X H, et al. Numerical study on mechanism of explosive welding [J]. Science & Technology of Welding & Joining, 2012, 17(1): 36-41.
- [14] Wang X, Zheng Y, Liu H, et al. Numerical study of the mechanism of explosive/impact welding using Smoothed Particle Hydrodynamics method [J]. Materials & Design, 2012, 35: 210-219.
- [15] 王呼和, 佟铮. 平板金属爆炸焊接过程数值模拟 [J]. 焊接学报, 2010, 31(9): 101-104.
- [16] 张婷婷, 王文先, 魏屹, 等. 钛/铝/镁爆炸焊复合板波形界面及力学性能 [J]. 焊接学报, 2017, 38(8): 33-36.
- [17] Kahraman N, Gulenc B, Findik F. Corrosion and mechanical-microstructural aspects of dissimilar joints of Ti-6Al-4V and Al plates [J]. International Journal of Impact Engineering, 2007, 34(8): 1423-1432.
- [18] 胡赓祥, 蔡珣, 戎咏华, 等. 材料科学基础(第三版) [M]. 上海:上海交通大学出版社, 2000.

第一作者简介: 李岩, 1988 年出生, 博士, 副教授; 主要从事焊接工程与技术方面的科研和教学工作。

(编辑: 王龙权)

MAIN TOPICS, ABSTRACTS & KEY WORDS

Characteristics and causes of inertial friction welding defects between 2219 aluminum alloy and 1Cr18Ni9Ti stainless steel

Liu Zhao^{1,3}, Lan Ling², Wang Ting³, Zhang Ke¹, Jiang Siyuan³

(1. Shanghai Key Laboratory of Materials Laser Processing and Modification, Shanghai Jiao Tong University, Shanghai 200240, China; 2. Shanghai Shipbuilding Technology Research Institute, Shanghai 200032, China; 3. Shandong Provincial Key Laboratory of Special Welding Technology, Harbin Institute of Technology at Weihai, Weihai 264209, Shandong, China). p1 – 4

Abstract The joint of 2219 aluminum alloy and 1Cr18Ni9Ti rotary body was connected by inertial friction welding technology. The microstructure and defects of the welded joint were analyzed by SEM and EDS. The results showed that the lamellar microstructure parallel to the weld interface formed on the side of the aluminum alloy, including equiaxed fine grain area formed by dynamic recrystallization and deformable grain area elongated along the direction of frictional shear. There were holes near the outer edge of the aluminum alloy side, Cu and O elements segregated around the holes. Brittle intermetallic compounds and oxides would cause stress concentration, hinder metal plastic flow and reduce joint performance. An intermetallic compound layer about 2 μm thick formed at the interface.

Key words: 1Cr18Ni9Ti stainless steel, 2219 aluminum alloy, inertial friction welding, hole defect, interfacial microstructure

Effect of assembling gap on formation and mechanical properties of joint by bobbin tool friction stir welding

Li Chong¹, Li Shuohan¹, Qi Zhenguo¹, Meng Xiangchen², Huang Yongxian²

(1. Hebei Jingche Rail Transit Vehicle Equipment Co., Ltd., Baoding 072150, Hebei, China; 2. State Key Laboratory of Advanced Welding and Joining, Harbin Institute of Technology, Harbin 150001, China). p5 – 9, 27

Abstract Bobbin tool friction stir welding (BT-FSW) was successfully utilized in the welding of aluminum alloy with hollow or sealed structures, while formation and mechanical properties of the joint were decreased by the manufacturing accuracy or assembling gap of the workpieces. Focusing on the problem, effect of the assembling gap (0 ~ 1.0 mm) on formation and mechanical properties of 4.0 mm thick AA6082-T6 BT-FSWed joint were investigated. The results indicated that with the increase of assembling gap, materials in the upper and bottom shoulders were not capable of filling the welds and voids defects were easy to occur in the bottom-shoulder affected zone under the effect of sucking-extruding, which decreased mechanical properties of joints. Formation and mechanical properties of the joint were superior under the assembling gap of 0 ~ 0.3 mm, tool rotational velocity of 700 r/min and welding speed of 300 mm/min.

Key words: T joint, bobbin tool friction stir welding, formation of joint, mechanical properties, assembling gap

Numerical simulation and experimental verification on forming mechanism of Ti/Al explosive welding interface

Li Yan^{1,2}, Li Yanbiao¹, Liu Cuirong¹, Ren Jinsuo², Zhao Rui²

(1. Taiyuan University of Science and Technology, Taiyuan 030024, China; 2. Shanxi Yangmei Chemical Machinery (Group) Co., Ltd., Taiyuan 030032, China). p10 – 15

Abstract Taking Ti/Al composite plate prepared by explosive welding as an example, the transient forming process of explosive welding was reproduced by numerical simulation, and the interface characteristics of explosive welding were analyzed by experiments. The results showed that interface morphology of Ti/Al composite plate changed from flat bonding to wave bonding along the propagation direction of detonation wave due to the penetration of jet. The lower pressure at the initiation point led to the boundary effect of explosive welding. The high impact pressure in the impact zone of explosive welding was the cause of plastic deformation and grain refinement near the interface. The interface defects of ex-

plusive welding were increased by high velocity impact, which provided a channel for the diffusion of atoms and realized metallurgical bonding. The results of numerical simulation were consistent with the experimental results, which revealed the forming mechanism of Ti/Al explosive welding interface.

Key words: Ti/Al composite plate, explosive welding, interface forming mechanism, numerical simulation

Laser ultrasonic detection for surface defect of stainless steel additive manufacturing parts

Fang Haiji^{1,2}, Ye Guoliang², Lü Bo¹, Zhang Yanxi¹, Gao Xiangdong¹

(1. Guangdong Provincial Welding Engineering Technology Research Center, Guangdong University of Technology, Guangzhou 510006, China; 2. Dongguan University of Technology, Dongguan 523000, Guangdong, China). p16 – 21

Abstract Laser ultrasonic technology was used to detect surface defects of the additive manufactured parts, and the finite element method was used to simulate the propagation process of laser-excited ultrasonic waves under the thermoelastic mechanism. The surface wave reflection signals received from different detection positions were analyzed, and the influence of the depth and width of defects on the surface wave reflection signal was studied. Laser ultrasonic testing experiments on 316L stainless steel additive manufacturing parts verified the correctness of the model, and then the wavelet soft threshold denoising algorithm was used to process the collected laser ultrasound signal. The results showed that the numerical simulation was basically consistent with the experimental results. The arrival time difference of the RS wave and the RR wave generated by the surface wave and the defect could detect the depth of defects, and the width of defects had almost no effect on the detection result.

Key words: laser ultrasonic detection, numerical simulation, surface defects, additive manufacturing

Interfacial microstructure and mechanical properties of copper/stainless steel fabricated by explosive welding

Jiang Chao¹, Long Weimin^{1,2}, Feng Jian³, Zhang Lei¹, Zhang Shuo²

(1. State Key Laboratory of Advanced Brazing Filler Metals and Technology, Zhengzhou Research Institute of Mechanical Engineering Co., Ltd., Zhengzhou 450001, Zhengjiang, China; 2. China Innovation Academy of Intelligent Equipment Co., Ltd., Ningbo 315700, Zhejiang, China; 3. Wugang Shenzhou Heavy Industry Clad Metal Materials Co., Ltd., Pingdingshan 462500, Henan, China). p22 – 27

Abstract T2 copper/06Cr19Ni10 stainless steel explosive welding clad plate was fabricated with welding parameters estimated by empirical formula. Interfacial microstructure and mechanical properties of copper/stainless steel clad plate were studied through optical microscope, scanning electron microscope, energy spectrum scanner, and mechanical test. It was founded that a regular wavy interface formed between copper and stainless steel after explosive welding. The interface was mainly solid-solid joining, and the discontinuous vortex-like cast microstructure was embedded in the wave peak and trough regions respectively. The microstructure was mainly composed of an ϵ -Cu matrix, γ -Fe precipitated phase, and stainless steel particles. Adiabatic shear band and austenite transformation were found in the microstructure of stainless steel after explosive welding. Annealing and recrystallization were observed in copper. Interfacial bonding strength was 280.3 MPa and microhardness of the microstructure near the interface was significantly improved. The maximum tensile strength of the clad plate was 561 MPa, mixed fracture characteristics were observed on the fracture of the bonding area, and the vortex microstructure defects had no obvious effect on the tensile fracture failure.

Key words: explosive welding, microstructure, mechanical properties, copper, stainless steel

Effect of laser incident angle on microstructure and mechanical properties of Ir-Rh alloy and Ni-based alloy by laser welding

Yang Huimu¹, Zhao Shifang², Hu Guoyi¹, Deng Jun¹, Du Dekui¹, Tao Wei¹

(1. Weichai Torch Technology Co., Ltd., Zhuzhou 412001, Hunan, China; 2. Central South University, Changsha 410083, China). p28 –